



Room 14-0551
77 Massachusetts Avenue
Cambridge, MA 02139
Ph: 617.253.5668 Fax: 617.253.1690
Email: docs@mit.edu
<http://libraries.mit.edu/docs>

DISCLAIMER OF QUALITY

Due to the condition of the original material, there are unavoidable flaws in this reproduction. We have made every effort possible to provide you with the best copy available. If you are dissatisfied with this product and find it unusable, please contact Document Services as soon as possible.

Thank you.

Some pages in the original document contain color pictures or graphics that will not scan or reproduce well.

Experimental Simulation of Wind Driven
Cross-Ventilation in a Naturally Ventilated
Building

by

Erin L. Hult

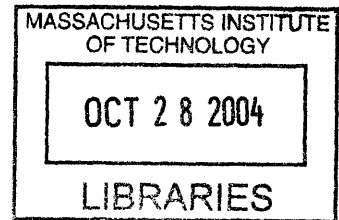
Submitted to the Department of Mechanical
Engineering in Partial Fulfillment of the
Requirements for the Degree of

Bachelor of Science

at the

Massachusetts Institute of Technology

[June 2004]
May 2004



© 2004 Erin Hult
All rights reserved

The author hereby grants to MIT permission to reproduce and to
distribute publicly paper and electronic copies of this thesis document in whole or in part.

Signature of Author.....
Department of Mechanical Engineering
May 7, 2004

Certified by.....
Leon R. Glicksman
Professor of Architecture and Mechanical Engineering
Thesis Supervisor

Accepted by.....
Ernest G. Cravalho
Chairman of the Undergraduate Thesis Committee

ARCHIVES

Experimental Simulation of Wind Driven
Cross-Ventilation in a Naturally Ventilated Building

by

Erin L. Hult

Submitted to the Department of Mechanical Engineering
on May 7, 2004 in Partial Fulfillment of the
Requirements for the Degree of Bachelor of Science in
Mechanical Engineering

ABSTRACT

A device was designed and constructed to simulate cross-ventilation through a building due to natural wind. The wind driver device was designed for use with a one tenth scale model of an open floor plan office building in Luton, England. The air flow patterns produced by the wind driver were observed, and the uniformity of the velocity of the flows into the model windows was measured for the three settings of the wind driver fans. The temperatures and velocities of flows on the interior of the building and at the exhaust windows were also examined.

The wind driver device was capable of producing uniform velocities across the face of the model to within 20 to 27%, depending on the fan setting. The consistency of certain features of the velocity distributions produced by the wind driver operating at different speeds suggest that improvements made to the design of the wind driver could lower this variation to about 15%. The velocities measured on the interior of the model seem consistent with interior velocities in the Luton building, although further experimentation is needed to confirm this trend. Cross-ventilation was effective in reducing interior model temperatures by up to 10°C from the natural convection case.

Thesis Supervisor: Leon R. Glicksman

Title: Professor of Architecture and Mechanical Engineering

Table of Contents

1. Introduction	6
1.1 Natural Ventilation of Buildings.....	6
2. Design of Wind Driver.....	7
2.2 Design Constraints	8
2.3 Design elements	9
2.3.1 Fans	9
2.3.2 Nozzle.....	10
2.3.3 Laminarizer.....	10
2.3.4 Positioning of device.....	10
3. Experimental methods.....	11
3.1 Inlet Velocity Testing.....	11
3.2 Outlet Flow Testing	11
3.3 Supply Air Temperature Testing	12
3.4 Interior Velocity Testing	12
3.5 Interior Temperature Testing.....	12
4. Results.....	12
4.1 Inlet Velocity Distribution.....	12
4.1.1 Wind Driver Location Testing.....	12
4.1.2 Average Velocity, Deviation and Error.....	13
4.1.3 Repeatability	14
4.1.4 Single Fan Velocity Distribution	15
4.1.5 Inlet Flow Visualization	15
4.2 Outlet Window Velocity Distribution.....	17
4.3 Outlet Window Temperature Distribution	18
4.4 Supply Air Temperature Distribution	19
4.5 Interior velocities	20
4.6 Interior Temperatures.....	21
5. Discussion.....	21
5.1 Inlet Velocity Distribution.....	21
5.1.1 Edge effects	22
5.1.2 Impact of Air Supply on Inlet Velocities	23
5.1.3 Variation due to single fan distribution.....	24
5.2 Outlet Flow Velocities	24
5.3 Outlet Temperature Distribution.....	24
5.4 Supply Air Temperature.....	25
5.5 Comparison with Observed Flows.....	25
5.6 Potential design improvements.....	25
5.6.1 Vibration of Wind Driver	25
5.6.2 Durability of Wind Driver	26
5.6.3 Fan Array Geometry.....	26
5.6.4 Nozzle Design.....	26
5.6.5 Laminarizer Length.....	26
5.6.7 Additional Baffles	27
6. Conclusions	28

7. Acknowledgments.....	28
8. References.....	29

Table of Figures

Figure 1: One tenth scale model of the Luton Building, prior to the installation of the atrium roof and the window awnings. The side on the right, with the window and vent openings is the south face.....	7
Figure 2: Model of the wind driver with detail of the honeycomb laminarizer.....	7
Figure 3: Floor plan of testing chamber, dimensions are in meters.....	9
Figure 4: Inlet velocity distribution (in m/s) at south face windows and vents for wind driver setting 3, average velocity = 3.6.....	13
Figure 5: Inlet velocity distribution (in m/s) at south face windows and vents for wind driver setting 2, average velocity = 3.0 m/s.....	14
Figure 6: Inlet velocity distribution (in m/s) at south face windows and vents for wind driver setting 1, average velocity = 2.25 m/s.....	14
Figure 7: Comparison of two inlet velocity tests at setting 3, in m/s.....	15
Figure 8: Velocity distribution for a single fan, setting 3.....	15
Figure 9: Cross-sectional view of flow based on velocity measurements between wind driver and model.....	16
Figure 10: Smoke trails illustrate flow from wind driver to the model and returning to the fan intake.....	17
Figure 11: Outlet window temperatures at north face windows and vents, fan setting 1.....	18
Figure 12: Outlet window temperatures at north face windows and vents, fan setting 2.....	18
Figure 13: Outlet window temperatures at north face windows and vents, fan setting 3.....	19
Figure 14: Inlet window temperature distribution for fan setting 2.....	20
Figure 15: Interior velocities at 3 fan settings at locations throughout the interior of the model.....	20
Figure 16: Interior temperatures averaged by floor and side of the model.....	21
Figure 17: Wind driver with additional baffles to reduce re-circulation from fan exit to fan intake.....	28

Table of Tables

Table 1: South face inlet window velocities, standard deviation of the velocity distribution across face and measurement error.....	13
Table 2: Exhaust flows at the north face windows and vents, velocity and deviation in m/s.....	17
Table 3: Average outlet temperatures at north face windows and vents by window row, temperatures in °C.....	19

1. Introduction

1.1 *Natural Ventilation of Buildings*

In particular environments, it is feasible to use natural ventilation to control the air flow and temperatures through a building. Natural ventilation utilizes flow produced either by natural convection currents or by forced convection due to naturally occurring winds to generate circulation in the building and regulate temperatures. The heating and cooling expense and energy that can be conserved by using natural ventilation techniques successfully is significant, and as a result, interest in building designs conducive to natural ventilation is increasing. Natural ventilation also has the potential to increase the air quality in a building. This is a particularly important function in large office buildings, where achieving high air quality tends to be difficult and employees may spend many hours at a time. The happiness and productivity levels of workers have been shown to be effected by the temperature and ventilation conditions in the work space.¹ In many effective designs, natural ventilation is used in conjunction with other green building methods, such as the storing heat in the thermal mass of the building in order to dampen the interior temperature oscillations due to the time of day.

In certain regions of the world, outside temperatures and wind conditions may be too extreme to allow for a comfortable interior conditions if natural ventilation is the sole source of ventilation. However, the implementation of passive cooling techniques such as daytime comfort ventilation and nighttime ventilation cooling provides an alternative to air conditioning in climates as hot and humid as Shanghai.² To maximize the range of conditions in which natural ventilation may be possible and to improve the design of buildings to maximize the use of this energy and health preserving measure, it is necessary to model the process of natural ventilation. Techniques such as computational fluid dynamics (CFD), on site measurements, and scale models using a variety of different fluids have been used in the modeling of naturally ventilated buildings.

1.2 *Modelling of Luton Building*

The building being modeled is an open floor plan office building in Luton, England. The Luton building was designed to be thermally controlled without the use of heating or air conditioning. The temperatures in the building are regulated by daytime ventilation and heat storage in the building's thermal mass to keep interior temperatures from falling outside the comfort range during cool nights. The air flows and temperatures in the building have been monitored in order to study the flow patterns in a successfully naturally ventilated building. The measurements were taken while the building was occupied, however, so extensive on site testing is not possible as it would be disruptive to the work environment in the building. A CFD model of the building has been developed to model the air flow and cooling of the Luton building. While CFD can be a very powerful tool in modeling natural ventilation, scale modeling can provide an alternative modeling approach. A one tenth scale model of the Luton building, shown below in Figure 1, has been constructed in order to model the different climate conditions that occur onsite in Luton.

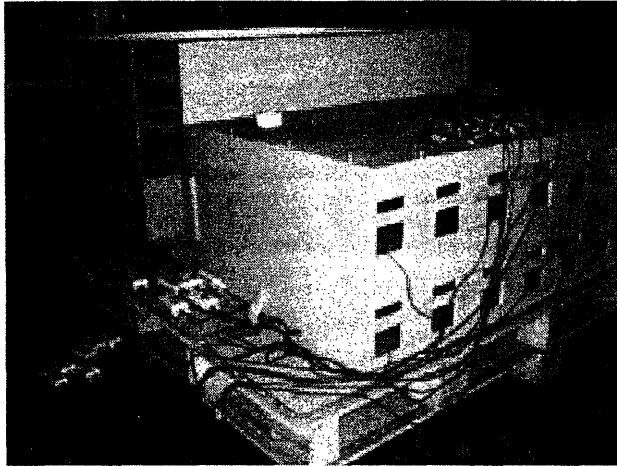


Figure 1: One tenth scale model of the Luton Building, prior to the installation of the atrium roof and the window awnings. The side on the right, with the window and vent openings is the south face.

Inside the building, temperatures and air velocities are monitored using thermocouples and mounted globe anemometers, described in further detail in Section 3. In order to use this scale model to model flows through the Luton building driven by outside winds, a device was needed to generate an even field of wind. The target wind speeds and direction of the wind were based on the conditions observed at the Luton building.

2. Design of Wind Driver

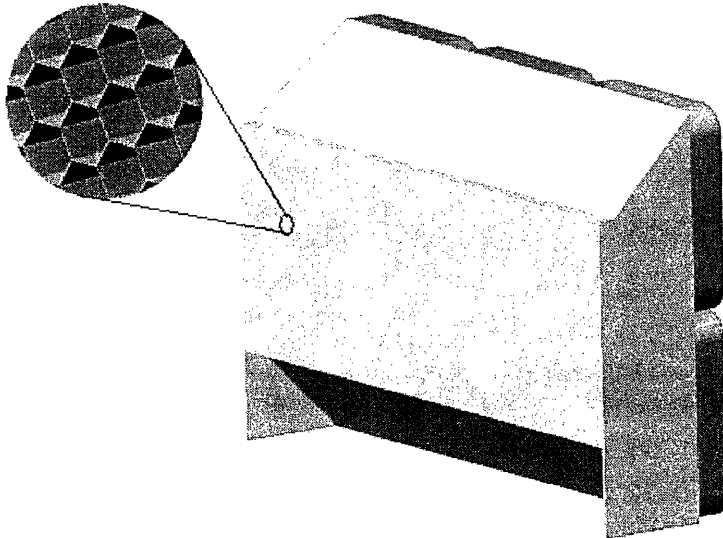


Figure 2: Model of the wind driver with detail of the honeycomb laminarizer.

2.1 Design Objectives

The purpose of this design was to create a device that would produce an air flow to simulate wind-driven cross-ventilation in a naturally ventilated building. The wind driver device was to simulate wind hitting the entire south face of the building. On the scale model, the south face of the building was 26" tall by 70" across. The device would ideally provide laminar air flow at the same velocity and temperature into each of the windows and vents on the south face of the model. Realistically, the target was to limit velocity variation to $\pm 1\text{ m/s}$ and temperature variation across the flow to $\pm 1.5^\circ\text{C}$. The device was to be able to provide air flow of at least three distinct speeds between 0 and 9 m/s, and was to be compatible with standard 3 prong plug, 120V power supply. The device was expected to be used for testing over the course of 6-12 months.

2.2 Design Constraints

The main constraint on the design of the wind generator was the amount of space between the model and the walls of the testing chamber. The model had to remain in the testing chamber and was essentially immobile due to its size, construction, and the testing instrumentation currently wired into the model. Between the south face of the model and the south wall of the chamber, there is 44" of space for the wind generator. There was enough space to place the fans at the north end of the chamber and design a duct to direct the airflow to the south flow of the model. However, because the cross-ventilation caused warmer air to be expelled out the windows at the north face of the model, if the fans were located nearby, the air blown into the model would have been at a temperature higher than the 'ambient' temperature. In order to minimize heat transfer from the northern exhaust to the fan-driven flow, the fans were best located on the south side of the building, adjacent to the chilled air diffuser. Cost was not a main constraint in this design, as time and ease of manufacture proved more significant than material costs.

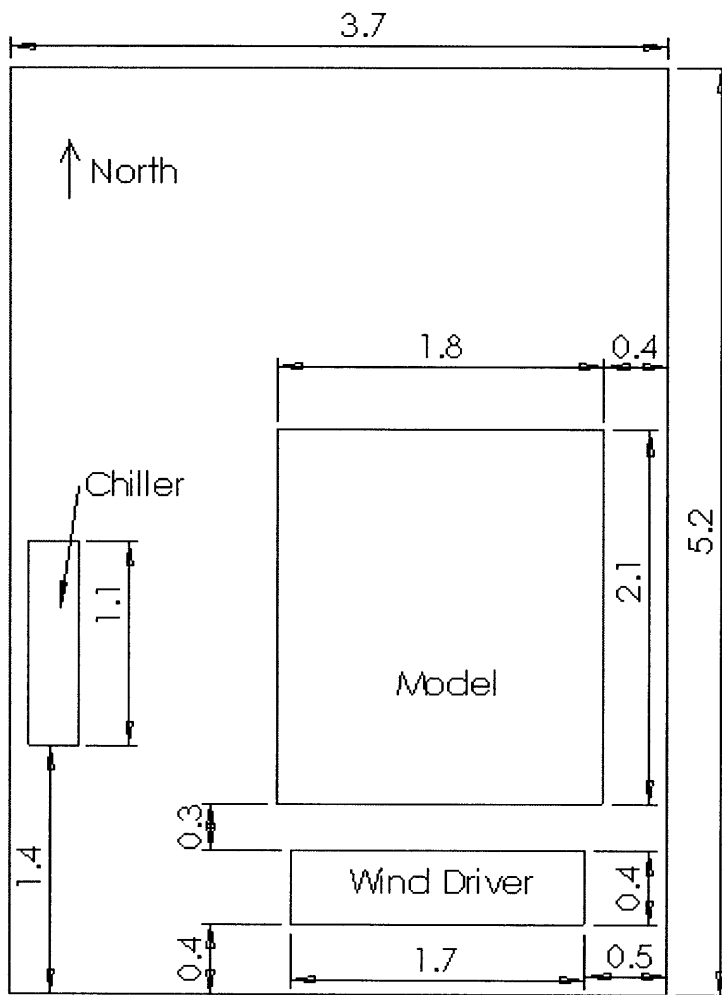


Figure 3: Floor plan of testing chamber, dimensions are in meters.

2.3 Design elements

2.3.1 Fans

To generate the necessary airflow, this design used six box fans mounted in an array, 3 fans across by 2 fans high. Each fan had a 20" blade diameter was quoted to provide air at 3 distinct settings: 4300, 3200, and 2100 cubic feet per minute. By mounting the fans adjacently in the array, the aim was that reduced velocities around the edges of a single fan would be increased by the additive effects of the neighboring fans. The metal box enclosures of these fans made it straightforward to connect several fans into an array. The relatively small thickness, 4.5", of this model made it a desirable choice, given the space constraints between the model and the chamber wall. Upon exiting the fans, the airflow enters the constricting nozzle.

2.3.2 Nozzle

The purpose of the nozzle is two-fold: to make the velocity profile from the wind generator more uniform and also to increase the volumetric flow rate of air to supplied to the model. Because of the reduction of the cross-sectional area of the generator duct between the face of the fans and the laminarizer, the bulk velocity of the airflow must increase, assuming density variation of the fluid is negligible. In order to maximize the velocity of the fluid leaving the duct, the shape of the duct must be carefully designed to minimize the drag on the fluid due to the duct geometry. In this design, the nozzle was constructed from foam core paper board. The top and bottom nozzle walls sloped inward forty-five degrees from the direction parallel to air flow to narrow the passage from 44" to 24" in height, as shown in Figure 2.

2.3.3 Laminarizer

The flow directly from the fans used is not laminar. The fans generate vortices and turbulent eddies due to the differential acceleration from the blades. In order to reduce the size of vortices and the degree of turbulence of the flow, the fluid is passed through a panel of individual channels. By reducing the cross-section of the flow from the entire duct to the diameter of an individual channel, the degree of turbulence of the flow is reduced. To reduce the vorticity of the flow due to the fan, the channel diameter must be significantly smaller than the fan blade diameter. The larger the ratio of panel thickness to cell diameter, the less turbulent the exiting flow, however the pressure drop associated with the flow through the panel increases with this ratio:

$$h_L = f (L/D)(V^2/2g) \quad (1)$$

where h_L is the head loss associated with the length, L , of the pipe. The laminarizer in this design consists of a honeycomb panel positioned at the exit of the nozzle. The honeycomb cell shape is clearly the preferred choice in devices designed to make flows laminar, as the shape has minimum perimeter to area ratio for a close-packed shape. The panel is two inches thick with one inch cell diameter and is made of phenolic-impregnated kraft paper. The disadvantages of using the kraft paper panel was that the panel was less stiff, less durable, and had higher surface roughness than similar panels made of plastic or metal. The higher surface roughness increases the drag on the flow and increases the transition Reynolds number for flow over the surface. The advantages to the kraft paper were easier machineability and lower weight than equivalent cell size plastic or metal honeycomb panels.

2.3.4 Positioning of device

In the experimental testing of the wind driver, it was determined that the positioning of the wind driver between the wall and the model significantly influenced flow rates into the model windows. When the wind driver is as close to the chamber wall as possible, maximizing the space between the model and the driver, the air flow to the rear of the fans is restricted, limiting the output of the fans. When the wind driver is located close to the model, the model wall acts in

reducing the flow velocities leaving the fan. Having the wind driver very close to the model also makes taking velocity readings at the window inlets very difficult. In addition to the magnitude of the velocity, the variation in velocity across the face also varies with the position of the wind driver with respect to the model. This change in variation of velocity with position may be linked to the tendency for the flow leaving the wind driver to circulate back to the fan intake and this is discussed in Section 5.1.2 Impact of Air Supply on Inlet Velocities.

3. Experimental methods

3.1 Inlet Velocity Testing

To get an indication of how uniform a wind the wind driver was providing the model, the velocity was measured at the inlet of each window and vent on the south face. The measurements were taken using a hand-held Control Company Traceable hot-wire anemometer. The anemometer resolution is 0.1 m/s for velocities in the range of 0.2 to 20 m/s, updating once per second. A time-average was approximated based on 10 seconds of observation at each point. To determine what distance between the driver provided the most uniform velocity field, tests were done at three locations. The resulting velocity fields were analyzed to give the final location of the wind driver. At the determined location, inlet window velocity testing was done two times for each setting of the fan.

Two tests were run to get an image of the flow fields in the region between the driver and the model. In the first test, vertical and horizontal velocity measurements were taken using the hand-held anemometer between the wind driver and the model. The measurements were taken every point on a 2 inch grid imposed on a vertical plane, parallel to the flow, at a location 16 inches in from the west edge of the south face. In the second test, smoke pencils were used to illustrate flow patterns in the space between the wind driver and the model. The resulting flows were sketched by hand.

The velocity distribution resulting from a single fan was measured, outside of the nozzle and laminarizer apparatus. Measurements of the flow normal to the fan face were taken on a 4 inch grid, 24 inches from the fan using the hand-held hot-wire anemometer.

3.2 Outlet Flow Testing

The exhaust flow velocities and temperatures from the model were measured at each of the windows and vents on the north face. The velocities and temperatures were measured using the hand-held hot-wire anemometer, for each of the three fan settings.

3.3 Supply Air Temperature Testing

The temperature was recorded at the inlets of each window on the south face at the intermediate fan setting to measure the temperature distribution of the supply air to the model. Temperatures were also recorded behind the fans at the air intake at 6 points.

3.4 Interior Velocity Testing

The cross-ventilation velocities on the interior of the model were measured using mounted globe anemometers and recorded using a digital sampling system and computer. The equipment sampled velocities continuously and recorded the velocity five times per second. Testing was performed at the three fan settings.

3.5 Interior Temperature Testing

The interior temperatures in the model were sampled continuously over a 20 minute period using Calibration T, 250 gauge wire thermocouples and a data logger. The thermocouples are rated to 0.4°F at 200.3°F The output from the data logger provided the temperature every 60 seconds. The thermocouples were located at 35 points throughout the building. Testing was done at three fan settings.

4. Results

4.1 Inlet Velocity Distribution

Inlet velocities were measured at each of the windows on the south face of the model. For each fan setting, window velocity measurements were taken twice.

4.1.1 Wind Driver Location Testing

The inlet velocities were measured with the wind driver positioned at different distances from the model to determine the most appropriate placement for the driver. At 20 inches from the model, the average inlet velocity was 2.9 m/s and the standard deviation was 1.5 m/s. At 16 inches, the average inlet velocity was 3.0 m/s and the standard deviation was 0.9 m/s. At 10 inches from the model, the average velocity was 3.6 m/s and the standard deviation was 0.7 m/s. Based on this information, the location of 10 inches from the model was chosen at which to perform the rest of the testing. In all sections to follow, the wind driver is positioned with 10 inches between the laminarizer exit and the south face of the model.

4.1.2 Average Velocity, Deviation and Error

Table 1 gives the velocities obtained at the inlet windows for the different fan settings.

Fan Setting	Average Inlet Velocity (m/s)	Standard Deviation (m/s)	Maximum Deviation (m/s)	Average Error (m/s)	Maximum Error (m/s)
1	2.2	0.5	1.3	0.3	0.7
2	3.0	0.8	1.9	0.3	0.9
3	3.6	0.7	1.5	0.4	1.4

Table 1: South face inlet window velocities, standard deviation of the velocity distribution across face and measurement error.

The velocity at each window is taken to be the average of the two measurements taken. The average inlet velocity for the fan setting is the arithmetic mean of the velocities at each window and vent. The standard deviation in Table 1 is the standard deviation of the velocities from the average inlet velocity for the setting, and the maximum deviation is the maximum difference between a window velocity and the setting average. The average error is the average difference between the measurements obtained at the two trials at each window. The maximum error is the maximum difference between two velocity measurements taken at the same window.

The window locations in the following figures are not to scale, but give an indication of the velocity distribution for each fan setting and allow for visual comparison between multiple distributions. All velocities are in m/s.

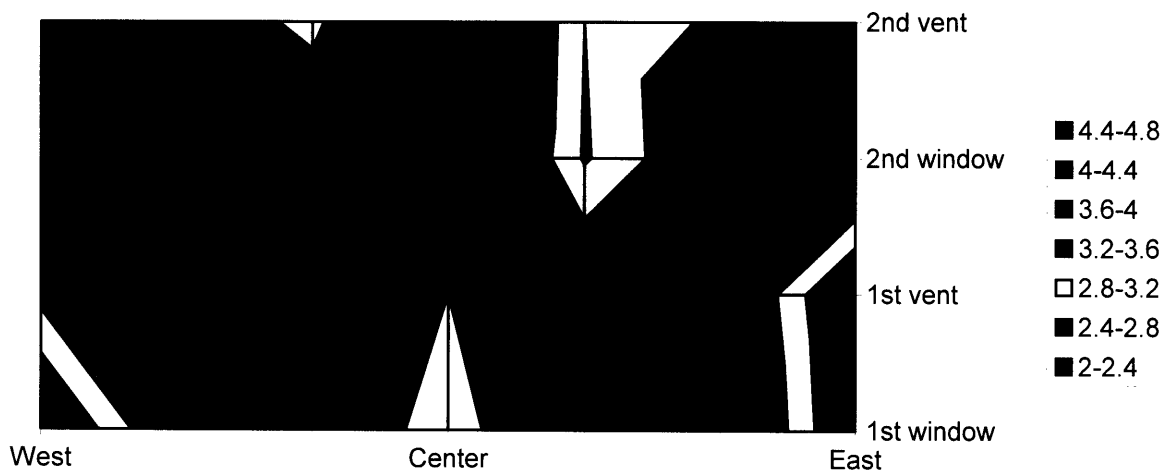


Figure 4: Inlet velocity distribution (in m/s) at south face windows and vents for wind driver setting 3, average velocity = 3.6.

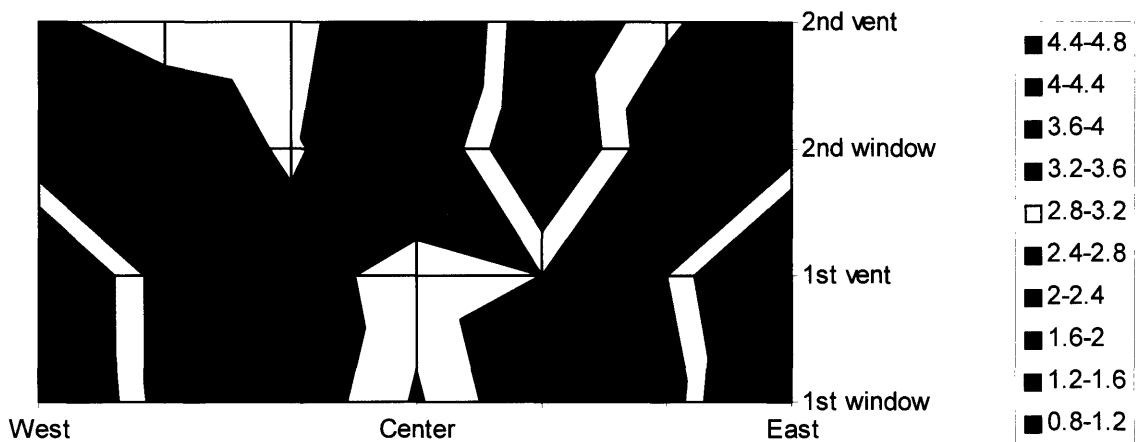


Figure 5: Inlet velocity distribution (in m/s) at south face windows and vents for wind driver setting 2, average velocity = 3.0 m/s.

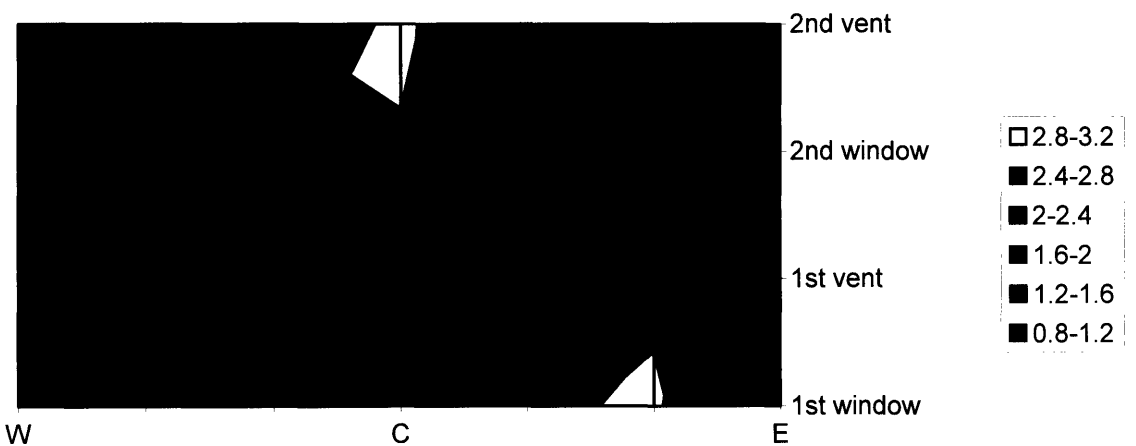


Figure 6: Inlet velocity distribution (in m/s) at south face windows and vents for wind driver setting 1, average velocity = 2.25 m/s.

4.1.3 Repeatability

The average error and maximum error values give an indication of the repeatability of the velocity distributions that were obtained.

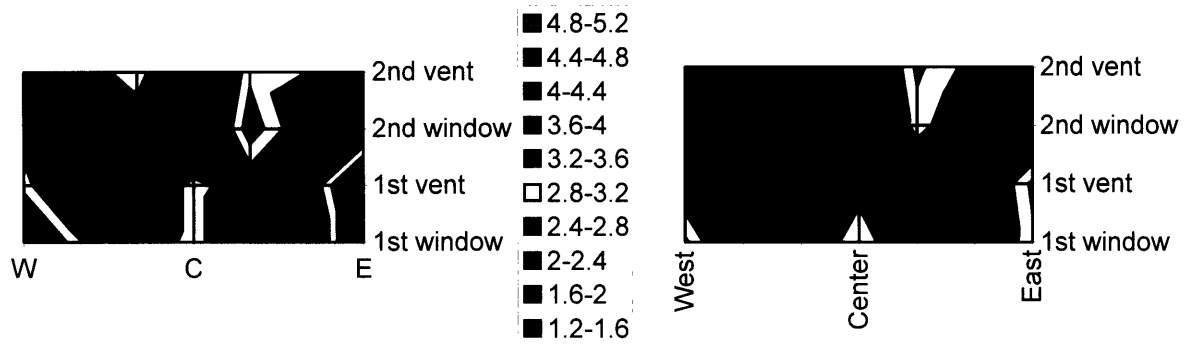


Figure 7: Comparison of two inlet velocity tests at setting 3, in m/s.

Comparing the two plots in the figure above provides a graphical means to compare the repeatability of two different velocity distributions obtained at the same wind driver setting.

4.1.4 Single Fan Velocity Distribution

The following figure gives the results for the single fan velocity testing as described in Section 3.1.

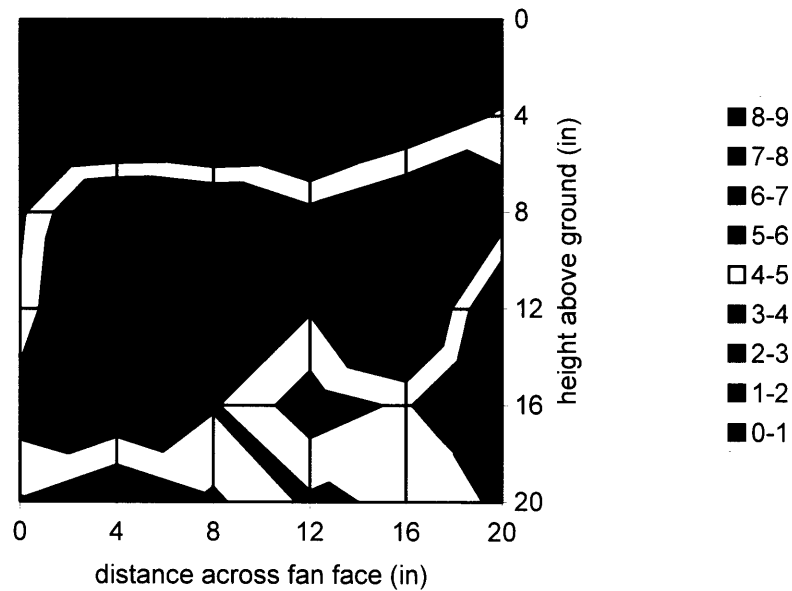


Figure 8: Velocity distribution for a single fan, setting 3.

4.1.5 Inlet Flow Visualization

The following images illustrate the air flow between the wind driver and the south face of the model.

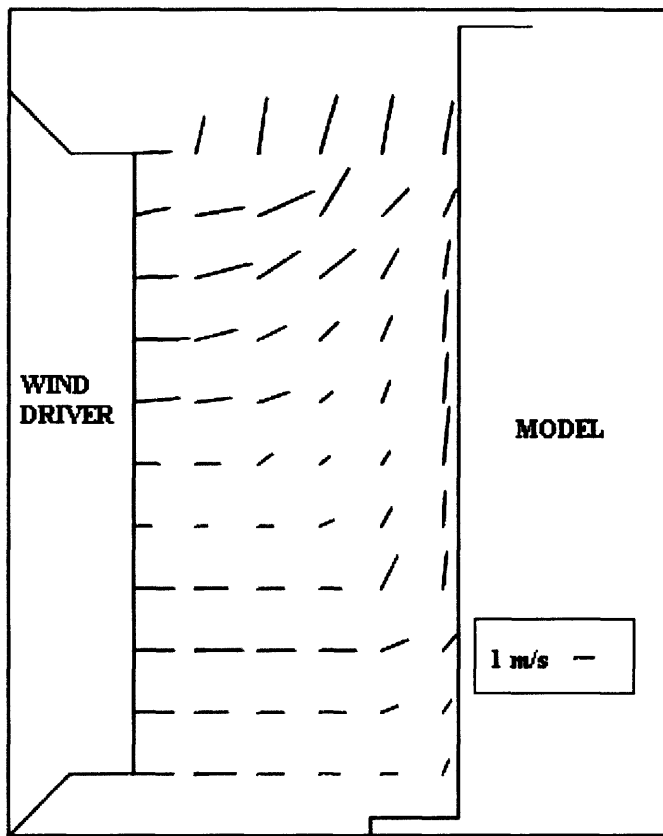


Figure 9: Cross-sectional view of flow based on velocity measurements between wind driver and model.

The results of the velocity measurements for flow visualization described in Section 3.1 are illustrated in Figure 9. The velocities in Figure 9 were obtained with the fan at setting 1, the lowest speed. The length of the velocity vector is proportional to the magnitude of the velocity in the plane shown at that point. Velocity normal to the plane shown is not represented in this figure. Smoke pencil tests indicated that after the air rose above the level of the model, a substantial amount of the air then flowed back over the top of the wind driver and into the fan intake to be re-circulated without ever having reached the model. The following image indicates a similar phenomenon occurring in the horizontal plane.

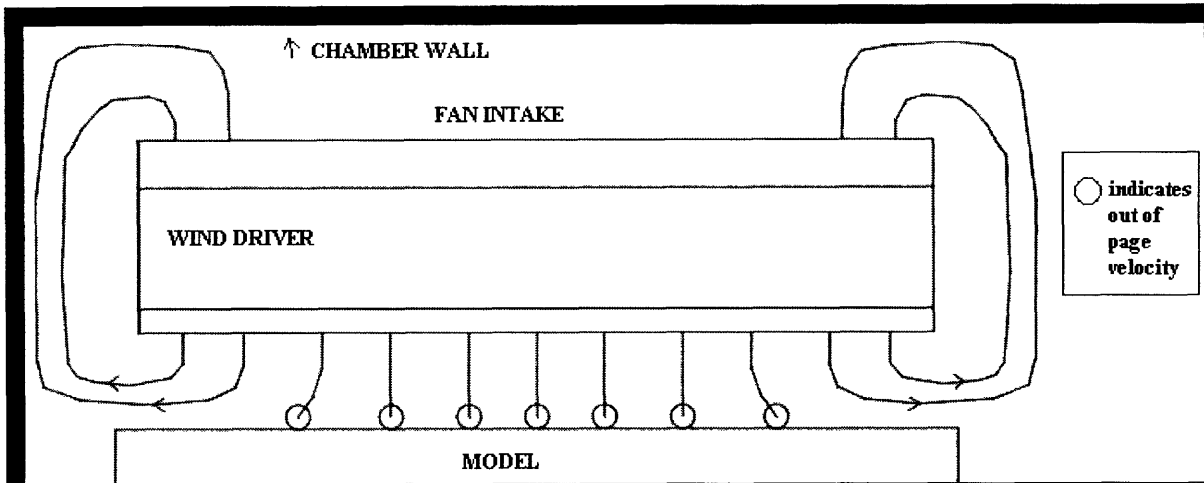


Figure 10: Smoke trails illustrate flow from wind driver to the model and returning to the fan intake.

The smoke trails in Figure 10 were observed at the height of the first floor windows. Due to turbulent mixing of the flow, at some points the precise path of the flow could not be seen, but the flow typically was normal to the fans at the center of the driver, and arced back to return to the fan intake towards the edges. At the points along the window face where windows existed, some of the flow would enter the windows, although those flows are not indicated on this figure, as that was not the dominant flow pattern observed.

4.2 Outlet Window Velocity Distribution

Outlet flow calculations follow the methods outlined for inlet velocity in Section 4.1.2.

Fan Setting	Average Outlet Velocity (m/s)	Standard Deviation (m/s)	Maximum Deviation (m/s)
1	1.1	0.1	0.3
2	1.5	0.3	0.5
3	2.2	0.2	0.4

Table 2: Exhaust flows at the north face windows and vents, velocity and deviation in m/s.

The fluctuations in temperature readings given by the anemometer were smaller and less frequent at the outlet windows than at the inlet windows.

4.3 Outlet Window Temperature Distribution

For these tests, interior heaters provided 300W to the building and the three vents in the atrium ceiling were closed. The following figures illustrate the trends in the exhaust temperature of air exiting the windows and vents on the north face of the model at the three fan settings.

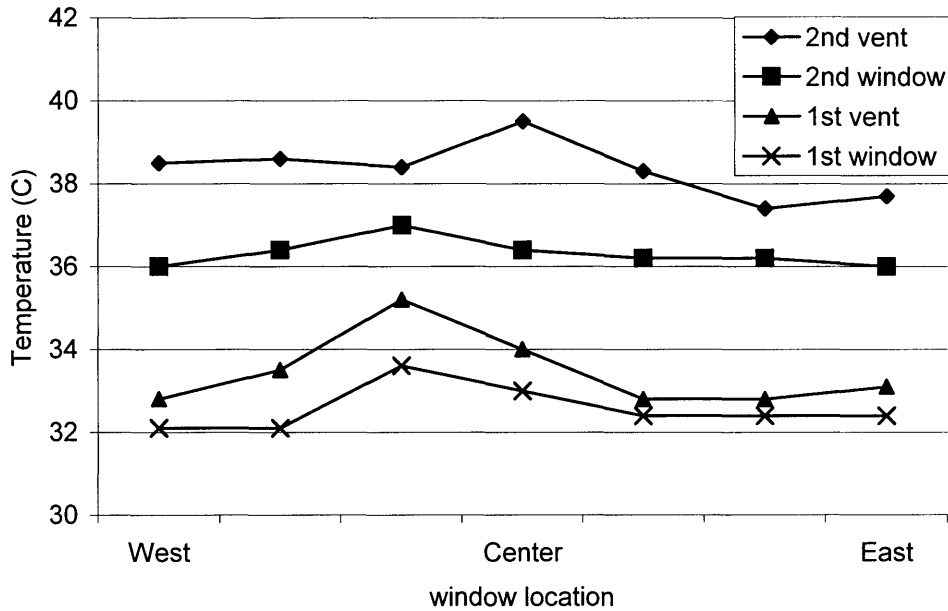


Figure 11: Outlet window temperatures at north face windows and vents, fan setting 1.

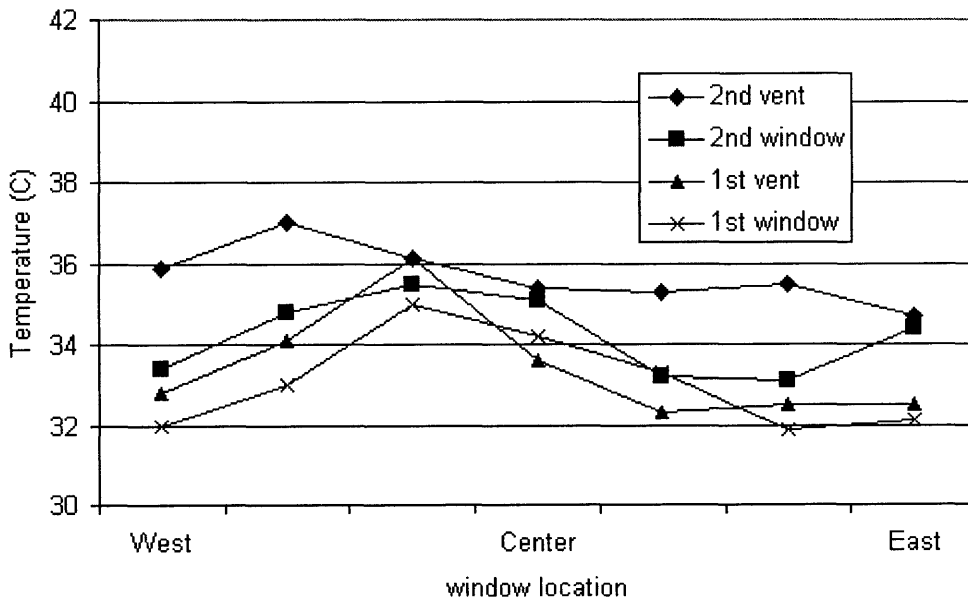


Figure 12: Outlet window temperatures at north face windows and vents, fan setting 2.

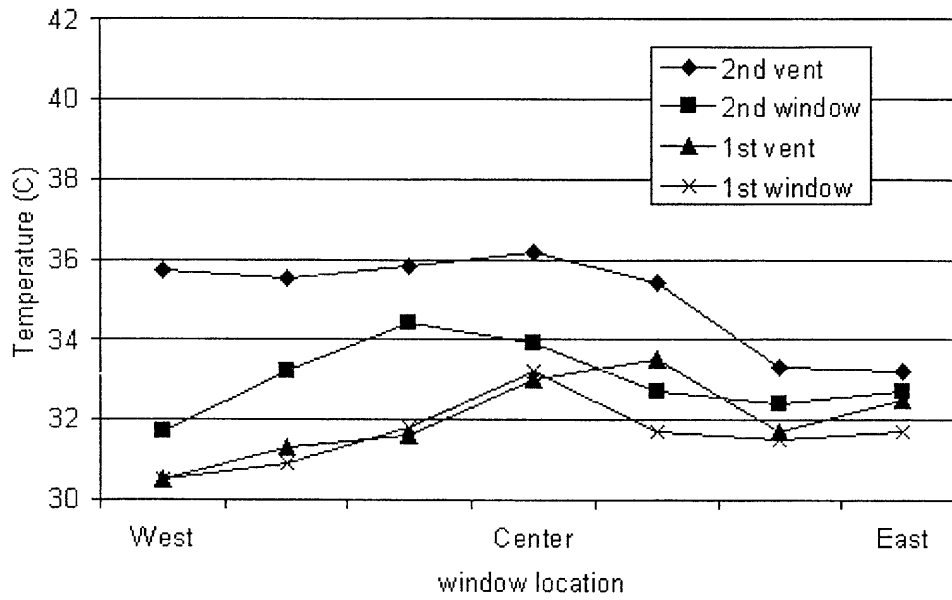


Figure 13: Outlet window temperatures at north face windows and vents, fan setting 3.

The following table gives the average temperature across each row of windows, for the three wind driver settings. The temperatures decrease as the fan speed increases.

Fan Setting	1 st Window	1 st Vent	2 nd Window	2 nd Vent
1	32.6	33.5	36.3	38.3
2	33.1	33.4	34.2	35.7
3	31.6	32.0	33.0	35.0

Table 3: Average outlet temperatures at north face windows and vents by window row, temperatures in °C.

4.4 Supply Air Temperature Distribution

The average temperature of the air entering the model was 26.1°C . The temperature of the air entering the model through the inlet windows is shown in the following figure.

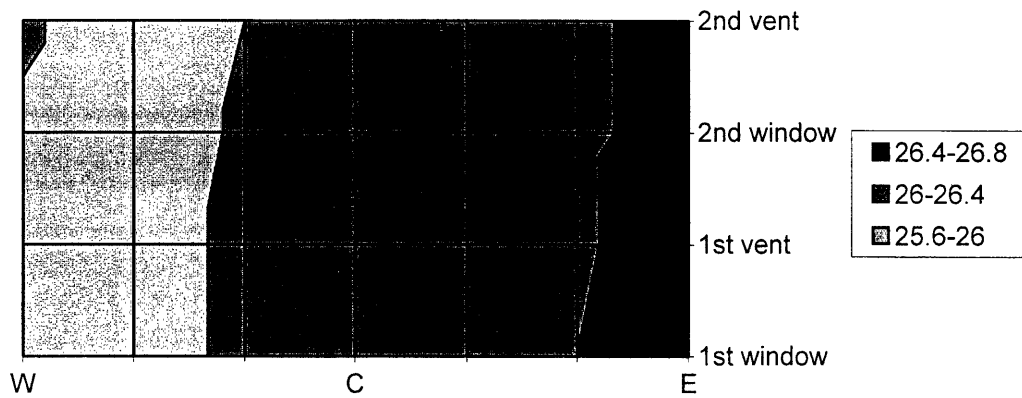


Figure 14: Inlet window temperature distribution for fan setting 2.

The temperatures measured at the fan intake reflected a similar distribution, with the highest temperatures, about 26.6°C, at the lower eastern-most locations, and the lowest temperatures, 25.5-25.6°C, along the western-most edge of the fan intake area. The air temperature entering the fan intake did not vary significantly with fan speed.

4.5 Interior velocities

The six data series seen in the following figure represent the velocities at points inside the model. The figure shows the moving average based on 250 data points for each series.

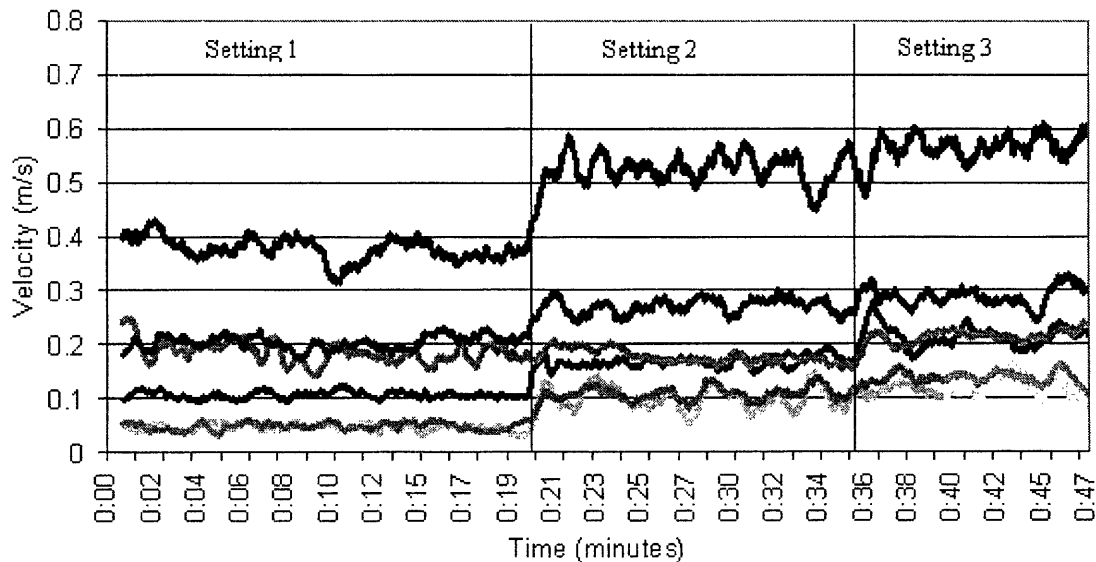


Figure 15: Interior velocities at 3 fan settings at locations throughout the interior of the model.

The setting of the fans was switched from 1 to 2 at minute 20 when equilibrium for setting 1 had been reached, and then was switched from setting 2 to 3 after equilibrium at setting 2 was reached at minute 35 of the test.

4.6 Interior Temperatures

The following figure shows the dynamic temperature response as the fan setting is increased from 1 to 2 to 3. Once the temperatures in the model had reached the equilibrium temperature for that setting, the wind speed setting was increased.

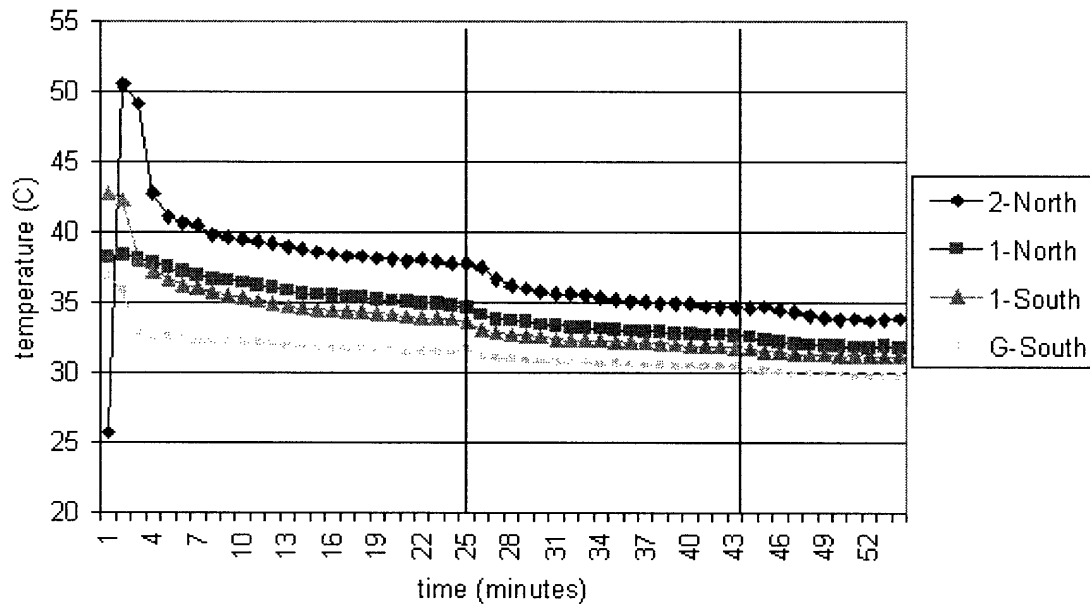


Figure 16: Interior temperatures averaged by floor and side of the model.

5. Discussion

5.1 Inlet Velocity Distribution

The ideal inlet velocity distribution would be uniform velocity across the face so that steady state measurements can be taken and evaluated. In the real case, the actual winds are not perfectly uniform, however, and neither were the winds generated in this experimentation. By looking at the velocity distributions obtained, it is possible to get a sense of how useful this device could be for simulating natural wind. Table 1 lists the average inlet velocities for the three fan settings. While uniform inlet velocities might not necessarily require uniform free-stream velocity, for this application, uniform inlet velocities is probably more important, as that is much of the flow that has been observed on site in Luton. For the three fan settings between 2.2m/s and 3.6m/s, the standard deviation from the average velocity varied between 0.5m/s and 0.8m/s. When the local fluctuation of wind speed at any given point is taken into account, this deviation is fairly

small. The average error indicates the typical difference between two measurements taken at the same location, which were 0.3 to 0.4m/s in these cases. Based on this data, it appears that this device is capable of producing a good approximation to natural wind.

By looking at the velocity distributions, however, consistent patterns appear in the data. Because velocity variations of fast or slow moving regions consistently appear in the same locations, regardless of the fan setting, there may be ways to alter the flow to correct for these variations. Since this larger scale variation does not seem to be random, the effects will not necessarily be negligible by repeating testing and averaging of results.

Looking at the velocity distributions in Figure 4, Figure 5, and Figure 6, the same pattern is clear in all three distributions. There exists a W-shaped field that is the highest velocity, with slow regions at the lower two corners, the bottom center, and at two intermediate points. A discussion of potential causes for the reduction of velocity at the corners follows in the next section.

5.1.1 Edge effects

Figure 5 and Figure 6 show significantly lower velocities at the west and east most columns of windows, specifically in the first floor window and vent. This effect is most noticeable at settings 1 and 2 (lower flow rates) but is also noticeable at the highest flow rate, as shown in Figure 4, setting 3. This could be due to reduced velocities produced at the edge of the fans that would be aligned with these windows, or due to the drag from the wall of the nozzle. A boundary layer thickness calculation can give an estimate for the thickness of the region affected by drag from the wall. For laminar flow, the correlation follows:

$$\delta/x = (30/R_x)^{-5} \tag{2}^3$$

Assuming an bulk velocity of 3.75 m/s, based on the velocities obtained at the highest fan setting, the Reynolds number based on the nozzle length is 6.0×10^5 , indicating the flow is likely to be turbulent. For turbulent flow, the correlation becomes:

$$\delta/x = 0.38/(R_x^{0.2}) \tag{3}^4$$

This correlation gives a boundary layer thickness of 1.1 cm, suggesting that boundary layer effects from the nozzle wall would not be a significant factor in reduced speeds at the edge windows and vents. The size of this boundary layer also suggests that boundary layer effects where the ground meets the edge of the model are also not significant, given that the distance between the ground and the first floor window is at least a factor of 10 greater than this expected boundary layer thickness. The insignificant size of the boundary layer suggests the cause may be more complicated. The reduced velocity at the edge effect is not visible in the second floor window and vent velocity measurements, suggesting variation may be due to other factors. For example, velocities might be higher on the second floor due to air flow patterns to the fan intake. The following section, Section 5.1.2, contains a discussion of the impact of the fan intake on the inlet flows.

5.1.2 Impact of Air Supply on Inlet Velocities

Disturbance to the air supply flow to the fan intake had the potential to produce a significant impact on the window inlet velocities. In order to measure window inlet velocities with a hand-held anemometer, it is necessary to stand within five feet of the measurement location.

Measurements taken while standing on the east side of the model varied in some cases quite significantly from measurements at the same window inlet, taken standing on the west side of the building. Measurements taken at windows on the east side of the south face seemed particularly affected by the location of the observer. With the fans on setting 3, with the wind driver positioned 16 inches from the model, the velocity recorded at specific windows while standing on the east side of the model was consistently three times the velocity measured standing on the west side. Specifically, in column 5, floor 2 window, the velocity was measured as about 2.8 m/s standing on the east side, and 0.9 m/s on the west side.

This variation seems to be related to the obstruction of airflow to the fan intake. Using foam core baffles to obstruct the flow toward the fan intake down the east side of the model, it was observed that such obstructions increase the velocities at some windows, while decreasing the velocities at others. Because of the smaller passage through which air can flow towards the intake, the velocity increases to maintain constant volumetric flow rates. However, the baffles seem to limit the overall volumetric flow rate of air that can reach the intake. For the window velocity results obtained in this report, no baffles were used, and all measurements were taken with the observer standing on the west side of the model, to keep the flow patterns as consistent as possible. If manipulation of specific window velocities is necessary, it may be possible to use a system of baffles to restrict flow intake to produce the desired output distribution, although this would require significant experimentation.

Perhaps the most significant indications of the importance of the patterns of air flow to the fan intake can be seen in Figure 9 and Figure 10, illustrating flows between the wind driver and the model. From the smoke trails and velocity measurements shown in these figures, it is clear that a significant amount of air is effectively drawn away from the model, over or around the wind driver and back into the fan intake. When Figure 10, smoke trails observed at the height of the first floor windows, is compared with the inlet velocity distributions seen at all three settings, the curvature of flows at the eastern most and western most corners of the south face correlates very well with the reduction of velocity of those flows. Because the flow at the corners is drawn back into the fan intake, the flow is deflected away from the direction normal to the model face, which would lower the inlet velocity at that location. This phenomenon is seen only at the bottom two rows of windows most likely because the air space between the ceiling and the wind driver is significant, whereas there is no gap between the wind driver and the floor for air to return to the intake.

The difficulty then becomes to modify the design to reduce the impact of the reverse flow back to the air intake on the inlet velocity distribution. Carefully placed baffles, forcing air to flow further away from the wind driver in order to return to the fan intake may be a potential solution. A shield to attempt to separate the wind flow to the model and the supply air intake flow would have to accomplish this task without restricting the flow from flowing around the edges of the model, as natural wind would tend to do.

5.1.3 Variation due to single fan distribution

In addition to the effects of the supply air flow to the impact, the distribution due to the geometry of the individual fans may play a role in the consistency of certain elements in the flow inlet velocity distributions. The geometry of the fan tends to concentrate the highest velocities in a ring around the center, leaving gaps at the edges, particularly at the corners, as well as at the center. Because the air flow from the fans passes through a nozzle which constricts the flow in the vertical direction, the variation in the vertical direction due to fan geometry may be negligible. Because there is no nozzle constriction in the horizontal direction, however, fan geometry may be causing the uneven distributions in the horizontal direction, particularly outside of the edge regions, which seem to be well explained by the impact of fan intake flows.

5.2 Outlet Flow Velocities

As seen in Table 2, the exhaust flow distribution is more even than the inlet flow distribution. This is expected, as the flow through the model acts as a flow straightener itself, and tends to even the flow as it passes through the building. There does not seem to be any discernable trends in outlet velocity, either with side of the building or the height or floor of the exhaust opening. The velocities at the different settings are approximately proportional to the inlet velocities at those settings, with the inlet velocity to outlet velocity ratio equal to 2.0 for setting 1 and setting 2, and 1.6 for setting 3.

5.3 Outlet Temperature Distribution

Figure 11, Figure 12 and Figure 13 illustrate the trends in outlet temperature distribution, by exit window level, and by fan setting. The stratification of flows by temperature as shown in the figures, with the hottest flows at the highest windows and floors is consistent with temperature distributions that have been observed with natural convection driving the ventilating flows, rather than forced convection. Variation in these temperature distributions across the face tend to be due to proximity to the point source heaters inside the model.

As the fan speed increases, the temperatures of the exhaust flows tend to decrease. These exhaust flow temperatures were recorded after the model had been given adequate time to adjust to the flow conditions and reach steady state temperatures. Because the higher velocities bring a greater volume of air through the model at a given time and the heaters are at constant power, the quantity of the heat that is transferred from the heater to a particular volume of air is lower at higher flow velocities. This effect is most visible, comparing the results from setting 1 and setting 2, or setting 1 and setting 3, as the difference between settings 2 and 3 is not as noticeable in these figures.

The outlet temperatures show similar stratification by floor as the interior temperatures, as shown in Figure 16.

5.4 Supply Air Temperature

From the results in Figure 14 for the inlet flow temperature distribution, the supply air is at an average temperature of 26.1°C, with an increase from 25.6°C to 26.8°C from the west side to the east side of the supply. While the temperature is probably close enough to uniform for the necessary precision of these experiments, the distribution could potentially be evened more by altering flow patterns from the exhaust or the diffuser. Cool air enters the room from the diffuser, the location of which is shown in Figure 3. Because of the proximity of the diffuser to the west side of the fan intake, there exists this slight temperature variation across the air flow to the model.

5.5 Comparison with Observed Flows

The velocities recorded at points in the interior of the model, shown in Figure 15, generally fall between 0.05m/s and 0.2m/s at the setting 1 and between 0.1m/s and 0.3 for settings 2 and 3. Velocities measured inside the Luton building were about 0.2m/s. In order to compare the interior velocities with interior velocities observed onsite in Luton, it is necessary to determine a scaling factor between these two velocities. Scaling analysis holding the Archimedes Number constant suggests that the velocity in the model should be equal to the velocity in the building. This suggests the wind driver is capable of simulating the interior velocities in the Luton building. This analysis involves the assumption that this scaling factor for buoyancy flow velocities will also be appropriate for forced convection velocities. In order to confirm this assumption, additional analysis is needed comparing the buoyancy velocity to forced convection velocity ratio in the building to that of the model. This analysis will also indicate how to scale outside free stream wind velocities to the appropriate wind driver produced velocities for the model.

5.6 Potential design improvements

Based on the results obtained in experimentation, as well as general observations of the wind driver device, a number of improvements are recommended to improve the performance and lifetime of the device.

5.6.1 Vibration of Wind Driver

One drawback of this design is that the nozzle and laminarizer tended to vibrate during operation. This phenomenon was most apparent at the highest fan setting, but is noticeable whenever the fans are in operation. The vibrations were reduced somewhat by attaching the laminarizer to the nozzle at more points, however the vibration still occurred. This vibration had two negative effects: it absorbed energy of the air flow and it weakened the wind driver structure over time. Using a honeycomb panel made of metal or plastic would give added stiffness to the structure and would likely reduce the amplitude of the vibrations. Increasing the thickness of the

panel or adding stabilizing supports at intervals across the laminarizer would also likely reduce the impact of the vibrations on the air flow.

5.6.2 Durability of Wind Driver

Because of the need to be able to move the wind driver device relative to the model, the device had to be durable. Due to the limited space between the model and the chamber wall, maneuvering the wind driver resulted in more wear to the device than the actual testing procedures. While the construction of the nozzle is sufficient to support the existing laminarizer under testing conditions, if the nozzle or the laminarizer were to be extended, additional structural supports would be needed to support the additional weight. Additional supports running from the lower to the upper wall of the nozzle would be helpful in not only supporting the upper wall, but also to provide additional mixing of the flows from the individual fans inside the nozzle. This additional mixing could help to make the velocity distribution resulting from the device more uniform.

5.6.3 Fan Array Geometry

Edge effects at the first floor windows may be reduced by increasing the size of the fan array. This could be accomplished by either adding additional fans to the array or adding spacers between the existing fans. Adding spacers would likely result in significant reductions in wind speed downstream of the spacers, unless the nozzle was modified to taper in both horizontal and vertical directions. The nozzle could also be lengthened to allow for more turbulent mixing to even velocities across the nozzle.

5.6.4 Nozzle Design

Reducing the angle of constriction in the vertical direction from 45 degrees to narrow the duct over a longer distance could have reduced the associated drag on the fluid. Any small curvature radius turn in a nozzle causes a significant pressure drop. Reducing this angle and rounding corners of the nozzle would serve both to increase wind velocities and to make the velocity profile of the air leaving the duct more uniform. The distance between the room wall and the model constrained the nozzle length and therefore the angle of constriction. Because this constriction in the vertical direction does appear to reduce local variation in the vertical direction due to fan geometry, such a constriction in the horizontal direction may also be beneficial to reducing similar variation in that direction. Depending on the degree of uniformity necessary as well as potential edge effect reducing improvements, this may not be necessary.

5.6.5 Laminarizer Length

One improvement of the design could be to increase the length of the laminarizer.

Despite the quality of the laminarizer, the diffuser needs to be improved in order to make the exit velocity more uniform across the flow. The laminarizer will not help to equalize the magnitude of air velocity normal to the model face. However, the laminarizer does serve to straighten the flow, reducing horizontal components of air velocity. Increasing the thickness of the honeycomb panel would help to force the exiting flow to be in the horizontal direction. Honeycomb panel manufacturers suggest a thickness to cell diameter ratio of at least 6 to 8 for normalizing of air flow direction.⁵ By calculating the entry length, x_e , necessary for the development of fully developed laminar flow in a pipe, it is possible to verify this ratio:

$$x_e / D \approx 0.03 Re_D \quad (4)^6$$

For the flow conditions through the laminarizer, Re_D is 4500, so this relation suggests an entry length of 3.4 meters. Based on this result, the flow exiting such a honeycomb panel will not be fully developed laminar flow. However the Reynolds number is in the transition region, suggesting fully developed flow in a pipe may be turbulent. For fully developed turbulent flow of air through a pipe, entry length correlations become more involved, but an estimate for x_e / D of about 10 is suggested.⁷ This ratio correlates well with the estimate recommended by honeycomb panel manufacturers above. The required thickness of the panel will depend not only on this ratio, but also on the maximum pressure drop allowable over the panel, the effectiveness of the nozzle at pre-straightening the flow, and the allowable level of turbulence in the air provided to the model.

5.6.7 Additional Baffles

As discussed in Section 5.1.2 Impact of Air Supply on Inlet Velocities, constructing additional baffles may be useful in restricting flow exiting the wind driver from returning directly to the fan intake. When this flow from fan exhaust directly to fan intake occurs, there is increased variation in inlet velocities. Such baffles could extend from the wind driver structure, upward arcing over the flow exiting the fan, and on the sides of the wind driver, preventing flows from returning to the intake.

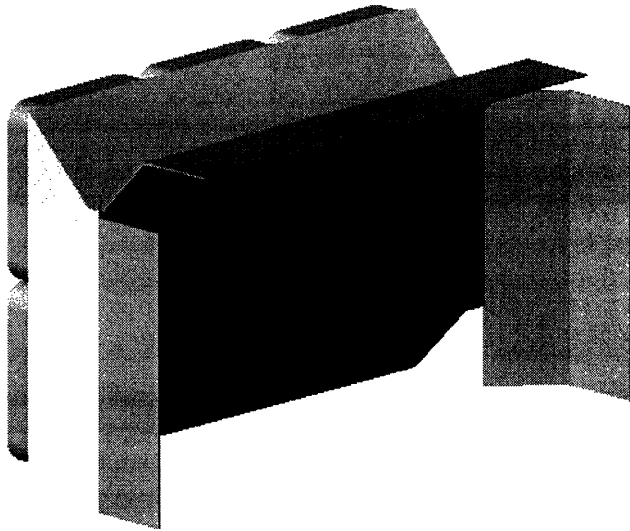


Figure 17: Wind driver with additional baffles to reduce re-circulation from fan exit to fan intake.

The potential effectiveness of such baffles in altering velocity fields should be tested before any significant features are constructed, as the impact may not warrant the time and effort to construct the device.

6. Conclusions

The wind driver device produced uniform velocities across the face of the model to within 20 to 27%, depending on the fan setting. The consistency of certain features of the velocity distributions produced by the wind driver operating at different speeds suggest that improvements made to the design of the wind driver could lower this variation to about 15%. The most important improvement that could be made to reduce the variation in velocities produced by the wind driver would be to construct additional baffles to prevent flow exiting the fans from returning directly to the fan intake. The velocities measured on the interior of the model seem consistent with interior velocities in the Luton building, although further experimentation is needed to confirm this trend. Cross-ventilation was effective in reducing interior model temperatures by up to 10°C from the natural convection case.

7. Acknowledgments

I would like to thank Leon Glicksman for his guidance and advice on this project. Thank you to Christine Walker for providing invaluable consultation on experimentation and documentation of this work. I would like to thank Richard Fenner for his advice on design of this device and Janelle Thompson for her advice on improving the design when its functioning was less than desirable. I would also like to thank Kristen Cook and Natalie Cusano for their willingness to

transport bulky items and help collect data and Darcy Kelly for her role in giving substance to this work.

8. References

- ¹ L. R. Glicksman and S. Taub, Thermal and behavioral modeling of occupant-controlled heating, ventilating and air conditioning systems. *Energy and Buildings*, 25 (1997) 243-249.
 - ² G. Carrilho da Graça, Q. Chen, L. R. Glicksman and L. K. Norford, Simulation of wind-driven ventilative cooling systems for an apartment building in Beijing and Shanghai. *Energy and Buildings*, 34 (2002) 1-11.
 - ³ J.K. Vennard and R.L. Street, *Elementary Fluid Mechanics*. John Wiley and Sons, New York, 1975.
 - ⁴ Vennard and Street, 1975.
 - ⁵ Hexcel Composites, Hexcel Corporation. Stamford, CT (2004). www.hexcelcomposites.com.
 - ⁶ F.M. White. *Viscous Fluid Flow*. McGraw-Hill Book Company, New York, 1974.
 - ⁷ J.H. Lienhard IV and J.H. Lienhard V, *A Heat Transfer Textbook*. Phlogiston Press, Cambridge, MA, 2002.
-